



Potential energy landscape of the $(\text{H}_2\text{O})_6^-$ cluster

Tae Hoon Choi, Kenneth D. Jordan *

Department of Chemistry and The Center for Molecular and Materials Simulations, University of Pittsburgh, Pittsburgh, PA 15260, United States

ARTICLE INFO

Article history:

Received 28 April 2009

In final form 26 May 2009

Available online 29 May 2009

ABSTRACT

Local minima and first-order saddle points on the potential energy surface of the $(\text{H}_2\text{O})_6^-$ cluster as described by a recently introduced one-electron model Hamiltonian are located using a combination of the basin-hopping Monte Carlo, doubly-nudged elastic band, and eigenvector-following methods. The minimum energy pathways connecting the transition states and minima are identified and used to construct disconnectivity diagrams. The implications of the calculated rearrangement pathways for experimental studies of $(\text{H}_2\text{O})_6^-$ are discussed.

© 2009 Elsevier B.V. All rights reserved.

1. Introduction

Negatively charged water clusters have been the subject of numerous studies [1–33] since their discovery mass spectroscopically in 1984 [34,35]. In recent years, vibrational predissociation spectroscopy [9–14] has provided considerable insight into the nature of the electron binding motifs of small $(\text{H}_2\text{O})_n^-$ clusters, and a large number of theoretical studies [15–33] have characterized selected local minima for these species. However, very little is known about the pathways for interconversion between different isomers, which has hampered interpretation of the experimental data. The main obstacle to computationally mapping out isomerization pathways of $(\text{H}_2\text{O})_n^-$ clusters has been the absence of a computationally fast, reliable method for exploring the potential energy surfaces. *Ab initio* methods cannot be used for this purpose, for any but the smallest clusters, due to the need to include electron correlation effects, preferably at the CCSD(T) level [36,37], and, at a minimum, at the MP2 level [38], together with the need to employ large, flexible basis sets.

Our group has recently introduced a one-electron polarization model (OEPM) [33] derived from our earlier Drude-model approach [27] for $(\text{H}_2\text{O})_n^-$ cluster systems. We have demonstrated that the OEPM approach gives electron binding energies and geometries of $(\text{H}_2\text{O})_n^-$ clusters in close agreement with the results of high-level *ab initio* methods. In a subsequent publication, we described the implementation of analytical gradients for the OEPM method [39], which means that we now have the computational tools for mapping out in detail the rearrangement pathways of $(\text{H}_2\text{O})_n^-$ clusters.

In this present study, we use the OEPM method to investigate the potential energy landscape of $(\text{H}_2\text{O})_6^-$. This cluster has been

chosen for study because it has been characterized experimentally by means of vibrational predissociation spectroscopy [10] and computationally by means of parallel-tempering Monte Carlo (PTMC) simulations [31]. In addition, it is the largest $(\text{H}_2\text{O})_n^-$ cluster for which the neutral precursor for the dominant form of the anion observed experimentally is known [11]. A combination of techniques, described in the computational methods section, are used to locate the local minima and first-order transition states and to map out the pathways between the transition states and local minima. These results are then used to express the potential energy landscapes in terms of disconnectivity graphs [40–42]. The experimental results for $(\text{H}_2\text{O})_6^-$ are discussed in light of the detailed knowledge of the potential energy surfaces gained in the present study.

2. Computational methods

2.1. Model potential

In the OEPM approach, the total energy of the water cluster anion is given by the sum of the energy of the neutral water cluster, described by the distributed point polarizable site (DPP) water model [43], and the electron binding energy (EBE) obtained from a one-electron model Hamiltonian, which includes the interactions of the excess electron with the point charges and the induced dipoles, as described by the OEPM model, as well as with the monomer-centered, short-range repulsive and polarization potentials [33]. The excess electron is described by a basis set of diffuse *s* and *p* Gaussians [29], and the polarization potential on each monomer is represented by a fit to a six *d*-type Gaussian functions centered at the *M* site of the DPP model to permit analytical evaluation of the resulting integrals. The OEPM model and the associated analytical gradients are described in Refs. [33,39], respectively.

* Corresponding author.

E-mail address: jordan@pitt.edu (K.D. Jordan).

2.2. Methods used to locate the stationary points

Basin-hopping Monte Carlo simulations [44–47] were used to locate a subset of the low-lying minima of $(\text{H}_2\text{O})_6^-$. This approach combines Monte Carlo walks and gradient based optimizations to locate local minima of the potential energy surface with Monte Carlo sampling being based on the energies of the optimized minima. A modified version of the limited-memory, quasi-Newton routine (LBFGS) of Nocedal and co-workers [48] was employed for the minimizations. The basin-hopping calculations were run for 4000 steps at a reduced temperature of 2.0 kJ/mol, the value used in an earlier study of protonated water clusters [47].

The low-lying minima found in the basin-hopping Monte Carlo calculations were used to initiate searches of transition states (TS) using the doubly-nudged elastic band (DNEB) procedure [49,50], followed by refinement of the TSs using the eigenvector-following algorithm [51–54], with the second derivatives being calculated by finite differences of analytical first derivatives. For each TS located, the minima to which it is connected were identified by LBFGS optimizations. Whenever these optimizations located a new local minimum, it was then used to initiate new TS searches. The transition states, minima, and the pathway information were used to conduct disconnectivity graphs [40–42] which provide a compact representation of the accessibility of different portions of the potential energy surface as a function of excess energy. The optimizations were done with the OPTIM program [55] which we interfaced with our OEPM code.

3. Results

A total of 266 minima and 469 transition states for $(\text{H}_2\text{O})_6^-$ were located. Essentially all the transition state structures and many of the local minima are new, *i.e.*, have not been previously reported in the literature. Fig. 1a shows the resulting disconnectivity graph

of $(\text{H}_2\text{O})_6^-$, and Fig. 1b presents a blowup of the low-energy portion of the graph containing 41 local minima. For each minimum in Fig. 1b, the magnitude of the electron binding energy (EBE) is indicated, and the binding motif is identified as AA or non-AA, where AA denotes structures with a double-acceptor water monomer with two dangling OH groups. The double-acceptor species are especially relevant as the dominant $(\text{H}_2\text{O})_6^-$ isomers observed experimentally fall in this class [10–12]. In addition, the minima are classified as book (BK), prism (PR), cage (CA), and open prism (OP) species. The OP isomers differ from the PR species in that they have one broken H-bond. This naming scheme follows that used in Ref. [31].

For the most part, the disconnectivity graph shown in Fig. 1a resembles a ‘palm tree’ in the terminology of Wales [41]. For an ‘ideal’ palm tree-type disconnective graph, efficient relaxation to the global minimum is expected [41,42]. However, for $(\text{H}_2\text{O})_6^-$ the two lowest energy minima, designated PR1 and CA1, are on different branches and are separated by a pathway with an overall barrier of ~ 7 kJ/mol, which makes their interconversion difficult at low temperatures. Only three of the 41 low-lying local minima have AA structures. These are denoted as OP1-AA, OP2-AA, and BK2-AA, and have calculated EBEs in excess of 400 meV. The observed vibrational predissociation spectrum of $(\text{H}_2\text{O})_6^-$ is due to the structurally similar OP1-AA and OP2-AA isomers (see Fig. 2) which are calculated to lie energetically about 5 kJ/mol above the non-AA CA1 and PR1 isomers. The remaining 38 low-energy minima have non-AA structures with low (≤ 250 meV) electron binding energies. The isomers labeled PR-N and BK-N have structures very similar to the neutral prism and book isomers, respectively, and EBEs ≤ 50 meV.

These results raise the question as to the nature of the minimum energy pathways connecting the low-energy AA and non-AA isomers. Moreover, since experimental studies have identified the neutral book isomer as the precursor to the observed AA anions

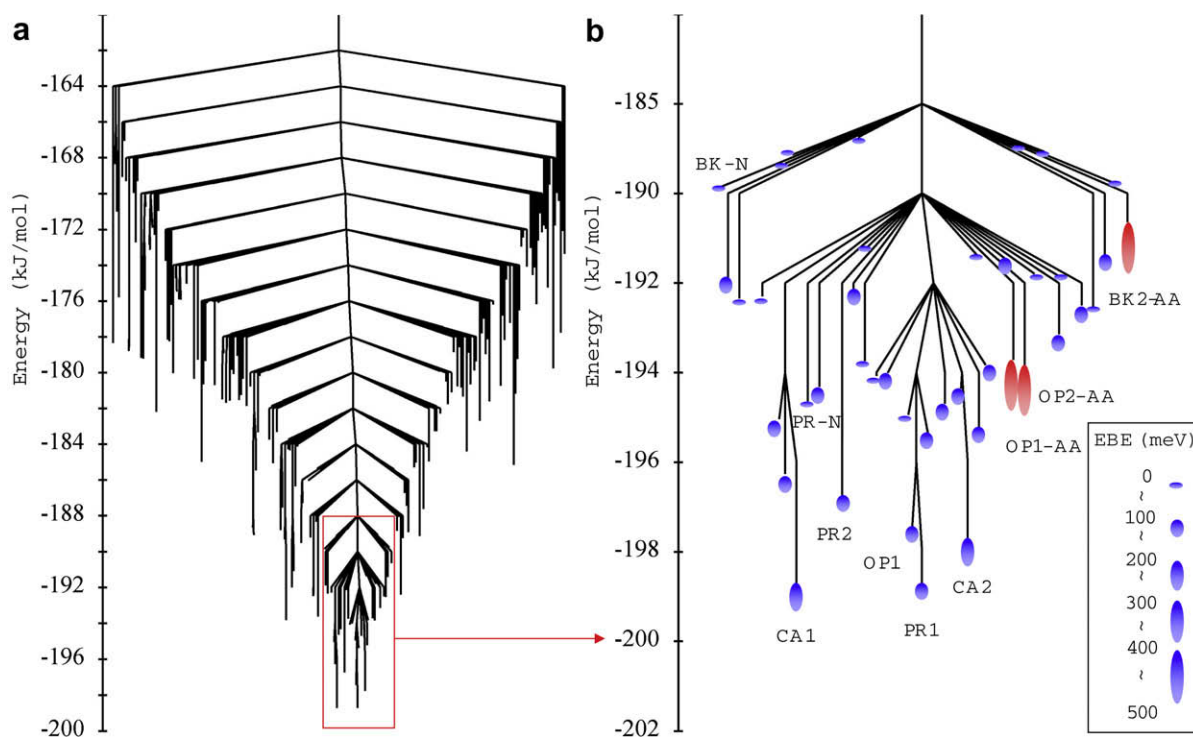


Fig. 1. Disconnectivity graph of the $(\text{H}_2\text{O})_6^-$ cluster: (a) disconnectivity graph of all stationary points identified in the work, and (b) an expanded view of the low-energy portion of the disconnectivity diagram. The oval figures indicate the magnitudes of the electron binding energies of the minima. Red and blue colors denote the AA minima and non-AA minima, respectively. (For interpretation of the references to colour in this figure legend, the reader is referred to the web version of this article.)

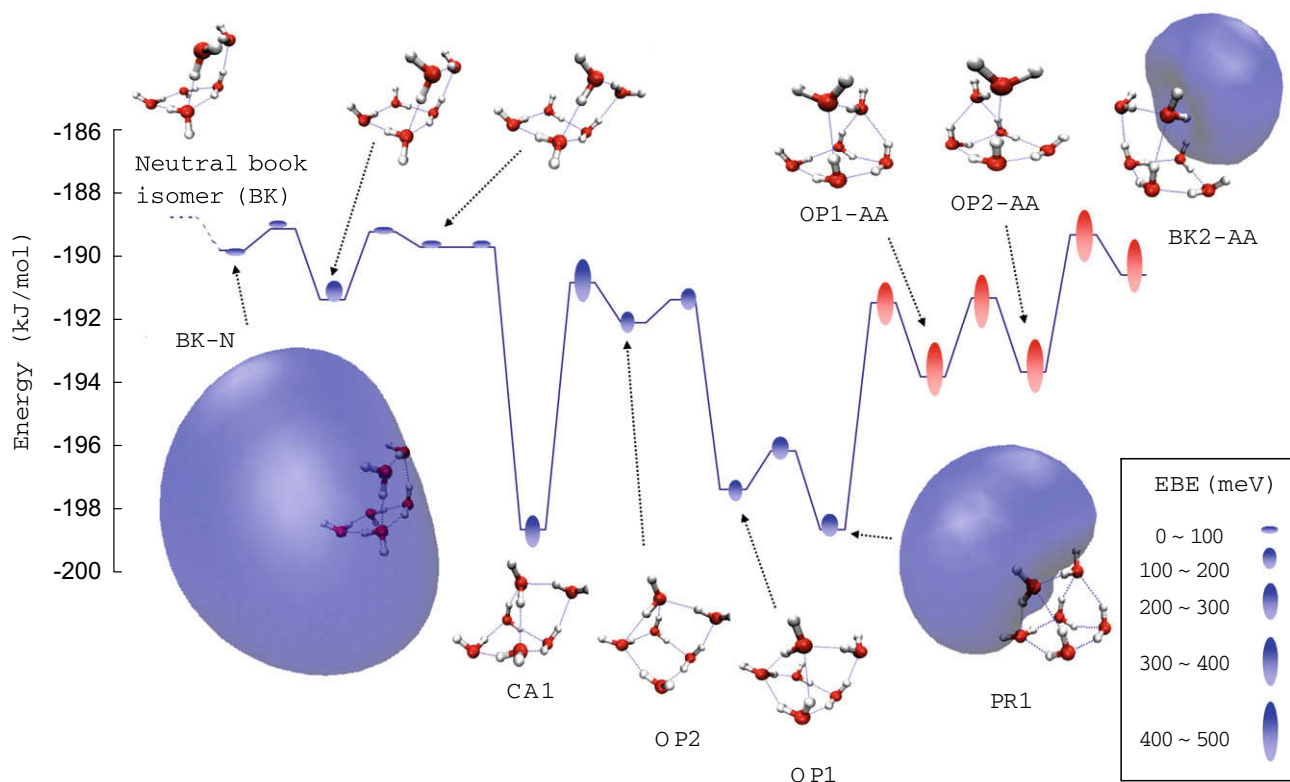


Fig. 2. The lowest energy pathway between the neutral book isomer (BK) and the OP1-AA, OP2-AA, and BK2-AA isomers of the $(\text{H}_2\text{O})_6^-$ cluster.

[11], it is also of interest to examine the minimum energy pathways from the neutral book isomer plus a free electron to the low-energy AA structures. The latter pathway, shown in Fig. 2, starts with a flip of a free OH group of the book form of the neutral cluster, giving the weak electron binding BK-N isomer, and then proceeds through the highly stable PR2, CA1, OP1, OP2, and CA2 non-AA species. In other words, the minimum energy pathway between the most stable AA and non-AA isomers of the anion occurs on the pathway from the neutral book to the AA species. The neutral book isomer has a dipole moment of 2.25 D and does not bind an excess electron in the OEPM model. (With a larger basis set this species would give very weak electron binding in the Born-Oppenheimer (BO) approximation [56], but probably would not bind the electron were non-BO corrections included.) The flip of one free OH group (see Fig. 2) causes the dipole moment to increase to 4.01 D, and the cluster (BK-N) now weakly binds the excess electron. The overall barrier to go from BK-N isomer to the OP1-AA and OP2-AA species is calculated to be only about 1.2 kJ/mol, and is due to a flip of a second free OH group; the overall barrier to go from the OP1-AA and OP2-AA species to the OP1 and PR1 non-AA species is calculated to be only 2.5 kJ/mol.

As seen from Fig. 2, OP1-AA and OP2-AA differ only in terms of which water monomer on the four-membered ring 'base' is H-bonded to the AA monomer in the water 'dimer' on top the tetramer. As a result, OP1-AA and OP2-AA have nearly the same energy and have very similar vibrational spectrum, and it is likely that both isomers contribute to the spectral signatures measured experimentally for the AA-type anion.

Thus far, we have focused on the pathways to go between geometrically distinct isomers of $(\text{H}_2\text{O})_6^-$. It is also of interest to examine pathways for scrambling of water molecules within the OP1-AA and OP2-AA isomers. Such rearrangement pathways are accessible experimentally by examining isotopologues such as $[(\text{H}_2\text{O})_5(\text{HOD})]^-$ or $[(\text{D}_2\text{O})_5(\text{HOD})]^-$ [57]. In Fig. 3a, we report one

such pathway for OP1-AA. The lowest energy pathway located goes through six intermediate local minima, including the highly stable PR1 and OP1 non-AA isomers. The overall activation energy for this process is calculated to be only about 3.1 kJ/mol, which means that it should be possible to drive the isomerization from OP1-AA or OP2-AA to PR1 and OP1 by excitation of an OH(OD) stretch or water bend vibration.

Given that the highly stable non-AA species are on the minimum energy pathways between the neutral book and the observed AA isomers, as well as for monomer scrambling in the low-energy AA species, it is surprising that only a small population of non-AA species is seen in the experiments of the Johnson group [10]. It may be that, following electron capture, the clusters do sample the highly stable non-AA isomers, but that the internal energies of these species are great enough that the resulting anions decay by electron ejection. This could occur by the anion exploring structures at which it lies energetically above the neutral cluster at the same geometry. This then raises the question as to how the cluster evolves from the neutral book isomer to the OP1-AA and OP2-AA isomers. The above analysis has focused on minimum energy pathways. Given the complexity of the $(\text{H}_2\text{O})_6^-$ potential energy surface, it is anticipated that there are many higher lying pathways, some of which may bypass the stable non-AA species and be less prone to electron autoionization. One such pathway is illustrated in Fig. 3b. This specific pathway has an overall activation energy of 17.6 kJ/mol, and, interestingly, goes through the 'tweezers' transition state which was first identified in the theoretical study of Kim and co-workers [18]. This particular pathway is probably not important experimentally, given the large barrier height, but is relevant as it indicates that there are indeed pathways that bypass the highly stable non-AA species.

It was noted in the introduction that the relative energies of different isomers of $(\text{H}_2\text{O})_6^-$ as described by the OEPM model closely reproduce those from high-level *ab initio* calculations [33]. We

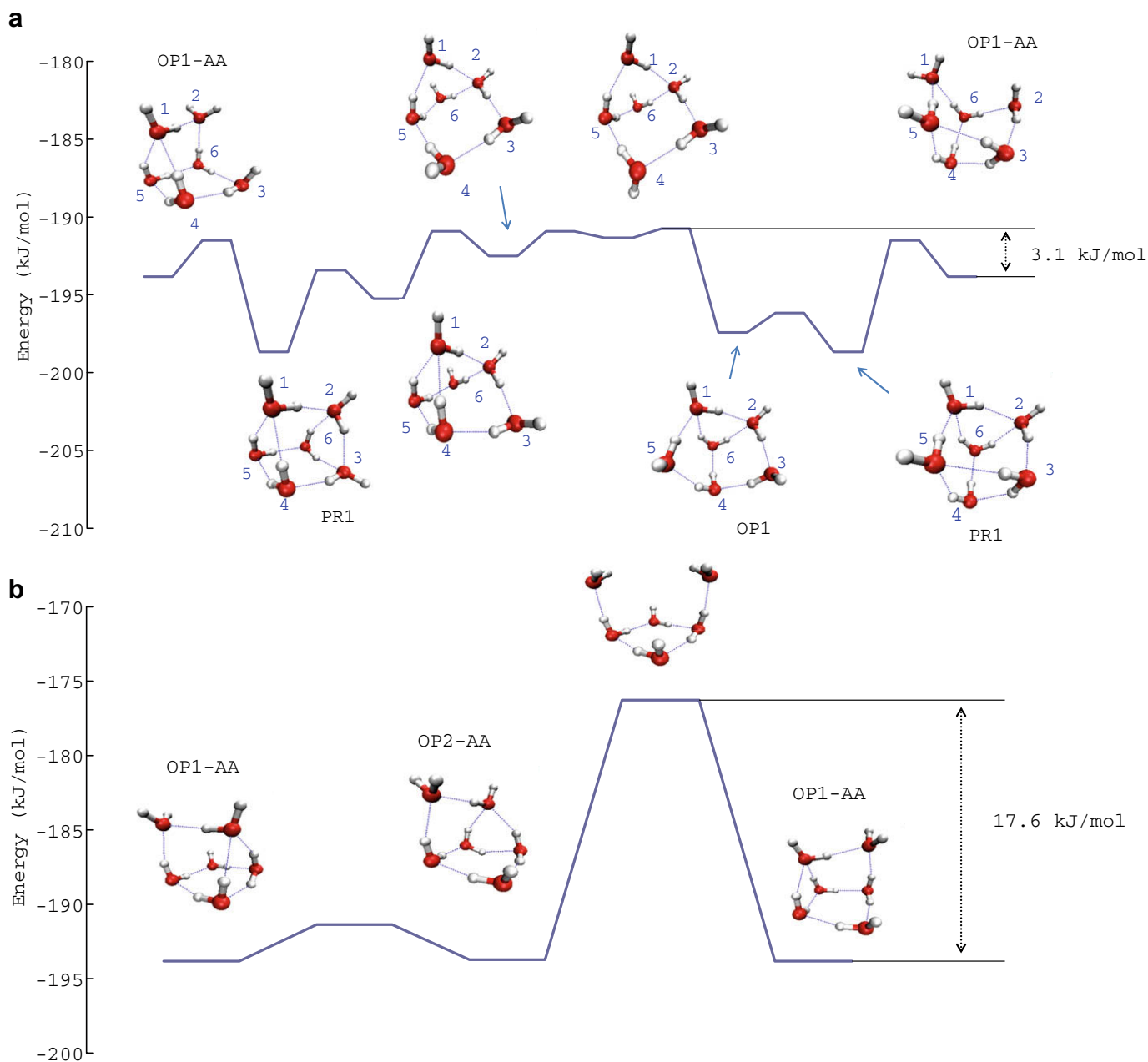


Fig. 3. Energy pathways for rearranging the OP1-AA isomer. (a) lowest energy pathway located; (b) example of a pathway that bypasses the highly stable non-AA isomers.

have also carried out *ab initio* calculations for selected transition states and find that the good agreement between the OEPM and *ab initio* results also holds for the activation energies. It is also important to consider whether inclusion of vibrational zero-point energy (ZPE) effects appreciably alters the relative energies of the isomers and the barriers for their interconversion. We find that although ZPE effects are important, e.g., lowering the energies between the AA and non-AA species, the disconnectivity graphs with inclusion of ZPE effects are qualitatively similar to those presented here and which ignore ZPE contributions.

4. Conclusions

In this work a one-electron polarization model was used to characterize the potential energy surface of $(\text{H}_2\text{O})_6^-$. The minimum energy pathway proceeding from the neutral book isomer to the

observed AA isomers proceeds through highly stable, but weak electron binding, non-AA species. Since non-AA species are not observed in high population in experimental studies, this result suggests that the highly stable non-AA species, if sampled following electron capture by the book isomer, may decay by electron detachment and that under experimental conditions the AA isomers may be formed via higher energy pathways that are less prone to electron detachment. Additional experimental and theoretical studies will be required to establish the detailed mechanism for formation of the AA anions in the case of $(\text{H}_2\text{O})_6^-$.

Acknowledgement

The authors acknowledge helpful discussions with Jing Ding and Drs. Revati Kumar, Mark Johnson, and David Wales. This research was carried out with support of a grant from the Basic Energy Sciences, Department of Energy.

References

- [1] K.S. Kim, I. Park, S. Lee, K. Cho, J.Y. Lee, J. Kim, J.D. Joannopoulos, *Phys. Rev. Lett.* 76 (1995) 956.
- [2] D.H. Paik, I.R. Lee, D.S. Yang, J.S. Baskin, A.H. Zewail, *Science* 306 (2004) 672.
- [3] N.I. Hammer, J.W. Shin, J.M. Headrick, E.G. Kiden, J.R. Roscioli, G.H. Weddle, M.A. Johnson, *Science* 306 (2004) 675.
- [4] K.D. Jordan, *Science* 306 (2004) 618.
- [5] D. Borgis, P.J. Rossky, L. Turi, *J. Chem. Phys.* 125 (2006) 064501.
- [6] J.V. Coe et al., *J. Chem. Phys.* 92 (1990) 3980.
- [7] J.R.R. Verlet, A.E. Bragg, A. Kammrath, O. Cheshnovsky, D.M. Neumark, *Science* 307 (2005) 93.
- [8] A.E. Bragg, J.R.R. Verlet, A. Kammrath, O. Cheshnovsky, D.M. Neumark, *Science* 306 (2004) 669.
- [9] N.I. Hammer, J.R. Roscioli, M.A. Johnson, E.M. Myshakin, K.D. Jordan, *J. Phys. Chem. A* 109 (2005) 11526.
- [10] N.I. Hammer, J.R. Roscioli, M.A. Johnson, *J. Phys. Chem. A* 109 (2005) 7896.
- [11] E.G. Diken, W.H. Robertson, M.A. Johnson, *J. Phys. Chem. A* 108 (2004) 64.
- [12] N.I. Hammer, J.R. Roscioli, J.C. Bopp, J.M. Headrick, M.A. Johnson, *J. Chem. Phys.* 123 (2005) 244311.
- [13] J.R. Roscioli, N.I. Hammer, M.A. Johnson, K. Diri, K.D. Jordan, *J. Chem. Phys.* 128 (2008) 104314.
- [14] J.R. Roscioli, M.A. Johnson, *J. Chem. Phys.* 126 (2007) 024307.
- [15] H.M. Lee, S.B. Suh, P. Tarakeshwar, K.S. Kim, *J. Chem. Phys.* 122 (2005) 044309.
- [16] S.B. Suh, H.M. Lee, J. Kim, J.Y. Lee, K.S. Kim, *J. Chem. Phys.* 113 (2000) 5273.
- [17] H.M. Lee, S.B. Suh, K.S. Kim, *J. Chem. Phys.* 119 (2003) 7685.
- [18] H.M. Lee, S. Lee, K.S. Kim, *J. Chem. Phys.* 119 (2003) 187.
- [19] A. Khan, *J. Mol. Struct.: Theochem* 850 (2008) 144.
- [20] M. Gutowski, P. Skurski, *Recent Res. Dev. Phys. Chem.* 3 (1999) 245.
- [21] M.J. Herbert, M. Head-Gordon, *J. Phys. Chem. A* 109 (2005) 5217.
- [22] M.J. Herbert, M. Head-Gordon, *Phys. Chem. Chem. Phys.* 8 (2006) 68.
- [23] R.N. Barnett, U. Landman, C.L. Cleveland, J. Jortner, *J. Chem. Phys.* 88 (1988) 4429.
- [24] L. Turi, W.S. Sheu, P.J. Rossky, *Science* 309 (2005) 914.
- [25] L. Turi, A. Madarasz, P.J. Rossky, *J. Chem. Phys.* 125 (2006) 014308.
- [26] T. Frigato, J. VandeVondele, B. Schmidt, C. Schutte, P. Jungwirth, *J. Phys. Chem. A* 10 (2008) 1021.
- [27] F. Wang, K.D. Jordan, *J. Chem. Phys.* 116 (2002) 6973.
- [28] F. Wang, K.D. Jordan, *J. Chem. Phys.* 119 (2003) 11645.
- [29] T. Sommerfeld, K.D. Jordan, *J. Phys. Chem. A* 109 (2005) 11531.
- [30] T. Sommerfeld, K.D. Jordan, *J. Am. Chem. Soc.* 128 (2006) 5828.
- [31] T. Sommerfeld, S.D. Gardner, A. DeFusco, K.D. Jordan, *J. Chem. Phys.* 125 (2006) 174301.
- [32] A. DeFusco, T. Sommerfeld, K.D. Jordan, *Chem. Phys. Lett.* 455 (2008) 135.
- [33] T. Sommerfeld, A. DeFusco, K.D. Jordan, *J. Phys. Chem. A* 112 (2008) 11021.
- [34] H. Haberland, H.G. Schindler, D.R. Worsnop, *Ber. Bunsen-Ges. Phys. Chem.* 88 (1984) 270.
- [35] H. Haberland, C. Ludewig, H.G. Schindler, D.R. Worsnop, *J. Chem. Phys.* 81 (1984) 3742.
- [36] J. Noga, R.J. Bartlett, *J. Chem. Phys.* 86 (1987) 7041.
- [37] K. Raghavachari, G.W. Trucks, J.A. Pople, M. Head-Gordon, *Chem. Phys. Lett.* 157 (1989) 479.
- [38] C. Møller, M.S. Plesset, *Phys. Rev.* 46 (1934) 618.
- [39] T.H. Choi, K.D. Jordan, *Chem. Phys. Lett.* 464 (2008) 139.
- [40] O.M. Becker, M. Karplus, *J. Chem. Phys.* 106 (1997) 1495.
- [41] D.J. Wales, M.A. Miller, T.R. Walsh, *Nature* 394 (1998) 758.
- [42] D.J. Wales, *Energy Landscapes*, Cambridge University Press, Cambridge, 2003.
- [43] A. DeFusco, D. Schofield, K.D. Jordan, *Mol. Phys.* 105 (2007) 2681.
- [44] D.J. Wales, H.A. Scheraga, *Science* 285 (1999) 1368.
- [45] J.P. Doye, D.J. Wales, *Phys. Rev. Lett.* 80 (1998) 1357.
- [46] J.P. Doye, D.J. Wales, *Phys. Rev. B* 59 (3) (1999) 2292.
- [47] T. James, D.J. Wales, *J. Chem. Phys.* 122 (2005) 134306.
- [48] R.H. Byrd, P. Lu, J. Nocedal, *SIAM J. Sci. Comput. (USA)* 16 (1995) 1190.
- [49] G. Henkelman, B.P. Uberuaga, H. Jónsson, *J. Chem. Phys.* 113 (2000) 9978.
- [50] S.A. Trygubenko, D.J. Wales, *J. Chem. Phys.* 120 (2004) 2082.
- [51] R.L. Hilderbrandt, *Comput. Chem. (Oxford)* 1 (1977) 179.
- [52] C.J. Cerjan, W.H. Miller, *J. Chem. Phys.* 75 (1981) 2800.
- [53] J. Simons, P. Jørgenson, H. Taylor, J. Ozment, *J. Chem. Phys.* 87 (1983) 2754.
- [54] L.J. Munro, D.J. Wales, *Phys. Rev. B* 59 (1999) 3969.
- [55] D.J. Wales, OPTIM: a program for optimising geometries and calculating pathways. <<http://www-wales.ch.cam.ac.uk/software.html>>.
- [56] M. Born, R. Oppenheimer, *Ann. Phys. (Leipzig)* 84 (1927) 457.
- [57] M. Johnson, Private communication.